EFFECTS OF HIGHLY CHARGED IONS ON COATED GLASSY CARBON.

[1]Innocent, A. J., [1]Ismail, M. Y. A., [2]Dawam, R. R., [2]Ike-Ogbonna, M. I., [3]Ponkin, D. and [3]Donets, E.
[1]Department of Physics, University of Pretoria, Hatfield, South Africa.
[2]Department of Physics, University of Jos, Jos, Nigeria.
[3]Laboratory of High Energy Physics, Joint Institute for Nuclear Research, Dubna, Russia.
Correspondence: joseph.innocent@fuhso.edu.ng +2348038428052.

ABSTRACT

The damage induced on glassy carbon coated with thin films of tungsten by slow, but highly charged ion, the Xe^{40+} of three different fluences and energies was studied and analysed. The pristine and irradiated glassy carbon coated with tungsten films were characterized at room temperature by Raman spectroscopy and atomic force microscopy. Raman results showed that the virgin glassy carbon has a crystalline size of 2.91 nm. This parameter was found to has reduce in size due to increase in disorder introduced by the HCI irradiation. The observed trends associated with irradiation, viz I_D/I_G reduction, upwards shift in D peaks, downwards shift in G peaks and increment in full width at half maximum FWHM in the HCI irradiated samples compared to the same parameters for the pristine glassy carbon, are signs of increase in the amount of disorder, which shows increase in the sp^3 content and bond-angle distortion induced by HCI irradiation on the same type of glassy carbon. This shows that W films play a shielding role, hence the glassy carbon structure suffers less disorder due HCI bombardment. Samples irradiated with high kinetic energy of 460 keV has the least crystalline size of 1.54 nm. This shows that the energy of HCI contributes substantially to damage introduced in the glassy carbon. The AFM results concur with the Raman results. The hillock size and surface roughness are most visible in the irradiated sample with largest energy of 460 keV. Glassy carbon enhanced with tungsten coatings could find applications in nuclear technology, especially for containment of dry nuclear waste.

Keywords: Glassy Carbon, HCI, Raman, AFM.

INTRODUCTION

Carbon exhibits great diversity due to strong dependence of its physical properties on the ratio of sp^2 to (Antunes, et al., 2006). There exist various types of sp^2-bonded carbons, with varying degrees of graphitic ordering, ranging from nanocrystals to glassy carbon. Carbon exists in many allotropic forms. In its natural form, carbon exists as amorphous carbon, graphite and diamond; carbon also exists in synthetic form as glassy carbon, fullerene, graphene, carbon nanotube, and more recently as carbyne which is believed to be the strongest material in the world (Mingjie, Vasilii , Hoonkyung, Fangbo, & Boris, 2013). Carbon is unique because a change in its local bonding can give rise to materials as diverse as diamond, graphite, fullerenes, carbon nanotubes, and disordered, nanostructure and amorphous carbons (Ferrari & Robertson, 2001). These materials have a remarkable range of mechanical, electronic, and electrochemical properties and many possible applications. The ability of carbon to exhibit various properties originates from the flexibility to form sp^1-, sp^2-, and sp^3-hybridized bonds (Meng, et al., 2017). Glassy carbon is a synthetic form of carbon formed by pyrolysis of organic resins at elevated temperatures (McCulloch, Prawer, & HofFman, 1994; Craievich, 1976). Glassy carbon exhibits a combination of glassy and ceramic properties with those of graphite materials - high thermal stability and does not transform into graphite even at high temperatures up to 3000 ^oC (Nathan, Smith, & Tu, 1974; Hlatshwayo, Sebitla, Njoroge, Mlambo, & Malherbe, 2017). Other properties of glassy carbon which suggest its suitability for use as radiation containment and encapsulation of spent nuclear fuel have been reported in (Innocent, et al., 2020), (Innocent, Hlatshwayo, Njoroge, & Malherbe, 2018). Tungsten (W) is a heavy metallic element,

a member of the third series of transition metals. Tungsten has the highest melting point of all metals, and at temperatures over 1650 ^{o}C has the highest tensile strength (Bukalov, Leites, Sorokin, & Kotosonov, 2014; Innocent, Hlatshwayo, Njoroge, & Malherbe, 2018; Philipps, 2011) have reported the properties of W which make it a candidate material for radiation shield.

The public perception of nuclear energy and it acceptance are low due to safety concerns with regard to storage and containment of the nuclear waste. This is a major scientific challenge which needs to be addressed through research to discover materials suitability and performance under irradiation. There is serious need for research on new material for extended service life of dry casks for nuclear waste storage, because the stainless steel, cast iron and concrete which are currently in use for making dry casks are susceptibility to corrosion and chemical attacks, which could ultimately lead to radiation leakage. Studies dealing with production of surface nano-structures on metals, semiconductors and insulators, upon bombardment with HCIs have been carried out by (Sobota, Pajek, Skrzypiec, Mendyk, & Teodorczyk, 2017), (Arnau, et al., 1997). Studies on the effects of highly charge ions on glassy carbon coated with tungsten is rare. Due to the properties highlighted in (Innocent, Hlatshwayo, Njoroge, & Malherbe, 2018), glassy carbon enhanced with tungsten coatings could find applications in nuclear technology, especially for containment of dry nuclear waste. It is therefore, pertinent to study its structural response to bombardment by highly charged ions. In order to have a better understanding of radiation effect on glassy carbon coated with tungsten as potential material for nuclear waste containment, the highly charged ions are used in this study to simulate the behavior of this material under irradiation. It is also believed that the results of this investigation will form important contribution to the ion-surface interaction database.

EXPERIMENTAL FRAMEWORK

The relative intensity of the D to G peaks (I_D/I_G) ratio for disordered graphite was found to be inversely proportional to the crystalline size (L_a) (Tuinstra & Koenig, 1970). With laser wavelength dependent constant denoted by (C_λ), this statement is mathematically expressed as

$$\frac{I_D}{I_G} = \frac{C_\lambda}{L_a} \qquad (1)$$

Equation (1) is valid for sp^2 bonded carbon materials within the range $2.5<L_a< 300$ nm for laser wavelengths of 488 and 514.5 nm (Tuinstra & Koenig, 1970). Using the peak intensity of D and G peaks extracted from the fitting, the I_D/I_G for pristine glassy carbon was estimated as 1.51. Substituting in Equation (1), intensity ratio and C_λ = 44 Å for the laser, L_a was calculated as 2.91 nm for the pristine glassy carbon. With increase in fluence of HCI, there is general decrease in the I_D/I_G. This downward trend in I_D/I_G with increasing fluence shows that the damage in the glassy carbon increases with fluence. This means that the irradiated glassy carbon samples suffers a loss of short-range order with reduce crystallite size. The reduced crystallite size is estimated from;

$$\frac{I_D}{I_G} = {L_a}^2\, C'(\lambda) \qquad (2)$$

where $C'(\lambda)$ = 0.0055 $Å^{-2}$ (Tuinstra & Koenig, 1970). The crystallite size of the irradiated glassy carbon samples are presented in Table 1. These values are smaller than 2.91 nm, calculated for pristine glassy carbon. This reduction in crystalline size confirms increase in disorder of the glassy carbon structure upon irradiation with HCI.

In the irradiated samples, Table 1 shows that D and G peak experienced slight shifts in peaks positions. D peaks of irradiated

samples shifted upwards in frequency relative to D peak position of 1350.3 cm^{-1} for pristine glassy carbon. It is observed that the sample irradiated with fluence of 5 × 10^{11} Xe^{40+}/cm^2 and kinetic energy of 460 keV experienced the maximum shift with D peak position of 1351.8 cm^{-1}. This could be attributed to the excess kinetic energy making it possible to cause large damage at a deeper depth in the structure of the glassy carbon. On the other hand, with the exception of sample GC 2.3, the shift in G peak is downwards with the irradiated sample at fluence 6.2 × 10^{11} Xe^{40+}/cm^2 and kinetic energy of 60 keV having the most downward shift of 1589.3 cm^{-1}. These observed trends associated with irradiation, namely; I_D/I_G reduction, upwards shift in D peaks, downwards shift in G peaks and increment in FWHM in the HCI irradiated samples compared to the same parameters for the pristine glassy carbon, are signs of increase in the amount of disorder i.e. increase in the sp^3 content and bond-angle distortion (McCulloch, Prawer, & HofFman, 1994), induced by HCI irradiation. The slight shifts in both D and G peaks are indicative that the damage induced in the glassy carbon due to HCI irradiation are at minima level compared to the results of ion implantation obtained by (Njoroge, et al., 2017) on the same type of glassy carbon. It shows that W films played a shielding role, hence the glassy carbon structure suffered less disorder due HCI bombardment.

MATERIALS AND METHODS

The type of glassy carbon used in this work and the detailed preparation of the coated samples were reported in (Innocent, et al., 2020), (Innocent, Hlatshwayo, Njoroge, & Malherbe, 2018). Slow, but highly charged ions (HCI) are characterized by high potential energy in the (keV) energy range (Sobota, Pajek, Skrzypiec, Mendyk, & Teodorczyk, 2017). The potential energy stored in HCI is the sum total of all the binding energies of the electrons removed from the atom (Das, Ohashi, & Nakamura, 2015), (Friedrich & Hannspeter, 2004). The interaction of HCI with a surface is dominated by the potential energy of HCI ions, which is deposited on a small surface area and along the first few nanometers below the target surface. With the currently available HCI sources such as electron beam ion traps (EBITs) or electron cyclotron resonance ion sources (ECRISs) or electron string ion sources (ESIS) (Aumayr, Facsko, El-Said, Trautmann, & Schleberger, 2011), it is possible to produce HCI beams, where the potential energy of the HCI exceeds their kinetic energy by far or at least dominates the interaction processes in a surface near region. In this study, the samples were irradiated with pure isotope ^{124}Xe (99,99%), produced by ESIS instrument at the Laboratory of High Energy Physics at Joint Institute for Nuclear Research, Dubna, Russia.

Raman spectroscopy is a scattering technique which is based on the Raman Effect. The signal of Raman spectrum is unique for a given material, hence results from Raman spectroscopy analysis are used to fingerprint materials (Raman & Krishnan, 1928). Raman spectroscopy is a standard non-destructive analytical technique largely used for the characterization of different carbon based material ranging from crystalline to amorphous carbons (Ferrari & Robertson, 2000), it is suited to detect the small change in the structural morphology of the carbon based materials. All the irradiated samples and the virgin glassy carbon were analysed using the Raman spectroscopy system at the department of Physics, University of Pretoria, Hatfield. Near surface optical microscopy such as atomic force microscopy (AFM), allows direct observation of solid surface at the level of

atomic scale (Schneider & Briere, 1996). This microscopy is suitable for surface defects investigation. The surface topographic modifications of the glassy carbon induced by Xe^{40+} ions were investigated using atomic force microscopy (AFM) housed in the department of Physics, University of Pretoria, Hatfield. AFM measurements of the studied samples were performed using a NanoScope V AFM equipped with NanoScope 8.10 software (Bruker-Veeco, USA). The images obtained were analysed on Nanoscope Analysis ver. 1.40 software (Veeco, USA). All the unambiguously identified features on the studied samples were separately investigated.

RESULTS AND DISCUSSION

Raman Results

Raman spectroscopy, due to its sensitivity to structural changes, is a powerful tool for monitoring changes in the microstructure of various carbon-based materials. In this study, Raman analysis was used to investigate the structural changes accompanying HCI irradiation on the W film-glassy carbon. Figure 1 shows the Raman spectrum with fitted simulation of pristine glassy carbon. A good fit on the Raman spectrum was achieved by using 4 Lorentzian and a Breit-Wigner-Fano (BWF) lines. The D peak was fitted with 3 Lorentzian lines, while a Lorentzian + BWF lines are sufficient to fit the G and D' peaks. The fitted Raman spectrum showed that the pristine glassy carbon spectrum is composed of two prominent peaks at 1350 and 1591 cm^{-1}. The peak at 1350 cm^{-1} is the called the disordered (D peak) which occurs in graphitic materials with small crystallite sizes similar to that reported by McCulloch, Prawer, & HofFman (1994). The peak at 1591 cm^{-1} (G peak) originates from lattice vibrations in the plane of the graphite-like ribbons present in the glassy carbon structure as those of McCulloch, Prawer, & HofFman (1994) and Elman, Dresselhaus, Dresselhaus, Maby, & Mazurek (1981). In addition to G peak, there is a presence of near the invisible small peak (D' peak) in Raman spectrum at 1621 cm^{-1} which appears as a shoulder on the G peak, it is attributed to small sp^2 crystallites in glassy carbon commensurate to Al-Jishi & Dresselhaus (1982).

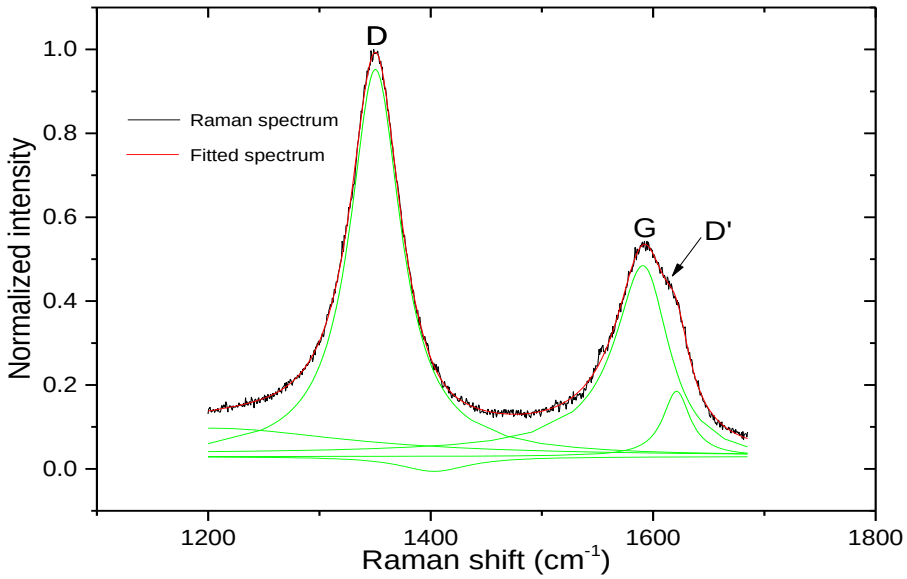

Figure 1: The Raman spectrum of pristine virgin glassy carbon (black line) fitted (red line) by four Lorentzian lines and a Breit-Wigner-Fano (BWF) line.

To explore the Raman results quantitatively, the spectra for all the irradiated samples were fitted in the same manner described above for pristine glassy carbon. Shown in Figures 2 and 3, are the Raman spectra of pristine glassy carbon and the samples irradiated with Xe^{40+} HCI. The fits to the Raman spectra using Lorentzian + BWF lines are also shown in Figure 3. The data extracted from the fits are presented in Table 1. The general trend observed in Figures 2, 3 and Table 1 is that, as the HCI fluence increases, the D and G peaks broaden due to an increase in disorder of the glassy carbon structure. These broadened peaks are quantified by their full width at half maximum (FWHM) as tabulated in Table 1.

In the in the irradiated samples, the D and G peak exhibit slight shifts in peak positions. D peaks of irradiated samples shift upwards in frequency relative to D peak position of 1350.3 cm^{-1} for pristine glassy carbon. The slight shifts in both D and G peaks are indicative that the damage induced in the glassy carbon due to HCI irradiation are at minima level compared to the results of ion implantation. In general, the observed trends associated with irradiation, viz I_D/I_G reduction, upwards shift in D peaks, downwards shift in G peaks and increment in FWHM in the HCI irradiated samples compared to the same parameters for the pristine glassy carbon, are signs of increase in the amount of disorder, which shows increase in the sp^3 content and bond-angle distortion induced by HCI irradiation on the same type of glassy carbon. This shows that W films play a shielding role, hence the glassy carbon structure suffers less disorder due HCI bombardment.

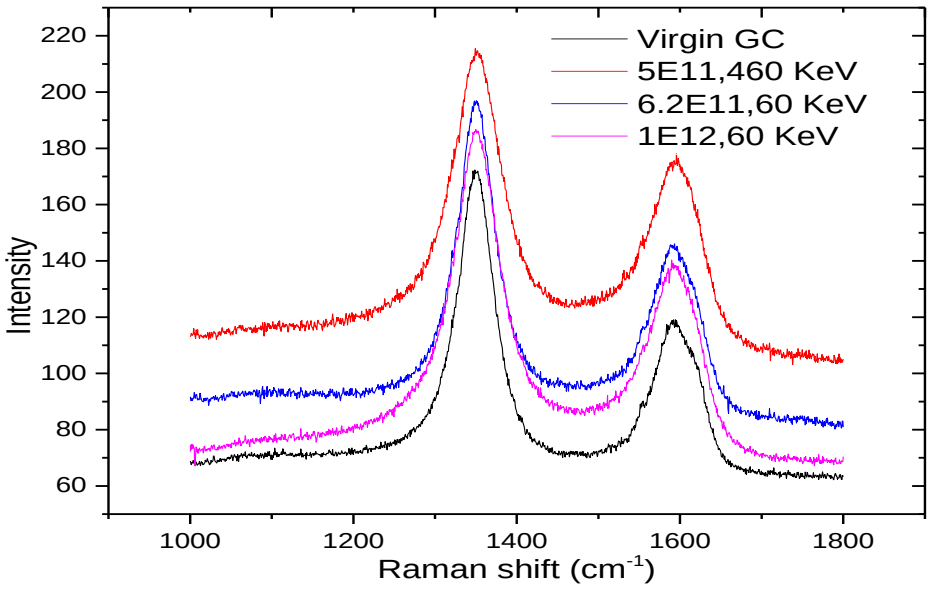

Figure 2: The Raman spectra of pristine and irradiated samples.

Table 1: Data extracted from the fitted Raman spectra of pristine glassy carbon and the irradiated samples.

Sample ID	φ (Xe^{40+}/cm^2)	E_K (keV)	I_D	I_G	I_D/I_G	L_a (nm)	D	G	D'
							FWHM (cm^{-1})		
VGC	0	000	0.923	0.611	1.511	2.91	55.6	59.8	29.8
GC 2.3	5.0E11	460	0.692	0.534	1.296	1.54	75.5	75.5	44.3
GC 2.1	6.2E11	060	0.789	0.556	1.418	1.61	56.6	62.7	37.9
GC 1	1.0E12	060	0.834	0.621	1.344	1.56	67.6	71.7	38.8

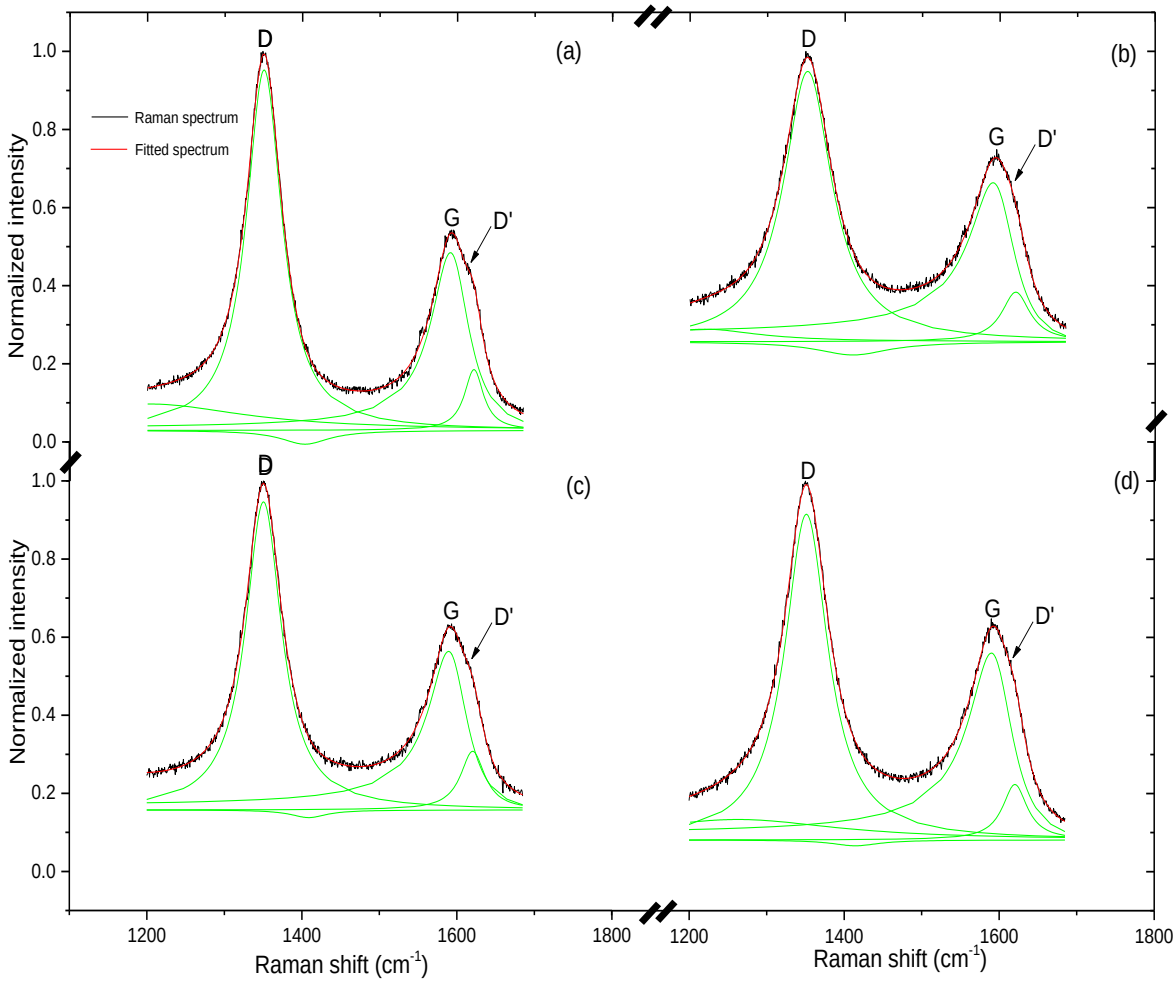

Figure 3: The Raman spectra of (a) pristine glassy carbon and samples irradiated with Xe^{40+} HCI of potential energy of 39 keV but with varying fluence and kinetic energy (b) fluence: 5.0 × 10^{11} ions/cm^2; E_k 460 keV (c) fluence: 6.2 × 10^{11} ions/cm^2; E_k 60 keV and (d) fluence: 1.0× 10^{12} ions/cm^2; E_k 60 keV.

AFM Results

To study the defects induced on the glassy carbon, the irradiated samples were observed under the atomic force microscopy (AFM). Figure 4 presents the AFM images obtained for pristine glassy carbon and irradiated samples. Figure 4 (a) reveals that the surface morphology of the pristine glassy carbon is fairly uniform, except for a line on it. Accidental scratch on the surface of the sample during handling is probably responsible for this line. In Figure 4 (b), the surface

morphology of the sample irradiated with HCI at fluence of 5.0 × 10^{11} Xe^{40+}/cm^2 and at kinetic energy of 460 keV appear very rough due to effect of high kinetic energy. The effect of this large kinetic energy resulted in surface sputtering of the sample, which eroded most of its surface defects with only few noticeable ones. The defect in this case is due to large dissipation of the kinetic energy of the HCI, similar to the feature observed by (Ferrari & Robertson, 2001). The nanostructures formed as results of HCI is observed to have increased in size with increase in fluence. This is true for Figures 4 (c) and (d) where the irradiated samples have the same kinetic energy of 60 keV but with different fluence of 6.2 × 10^{11} and 1.0 × 10^{12} ions/cm^2, respectively. The quantitative information on the characteristic features of the hillocks associated with each irradiated samples has been tabulated in Table 2. The development of hillocks with fluence and kinetic energy is clearly depicted by Figures 5, where hillocks height and size are shown below each of the 2D image. The cross-sectional view in Figure 5 shows that surface roughness is highest for irradiated sample at kinetic energy of 460 keV while it is least for the pristine glassy carbon sample. This remarkable difference in feature associated with Figure 4 (b) compared to Figures 4 (c) and 4 (d) also manifest in the Raman result. This shows that, the contributory effect of kinetic energy to surface defects induced by HCI cannot be ruled out.

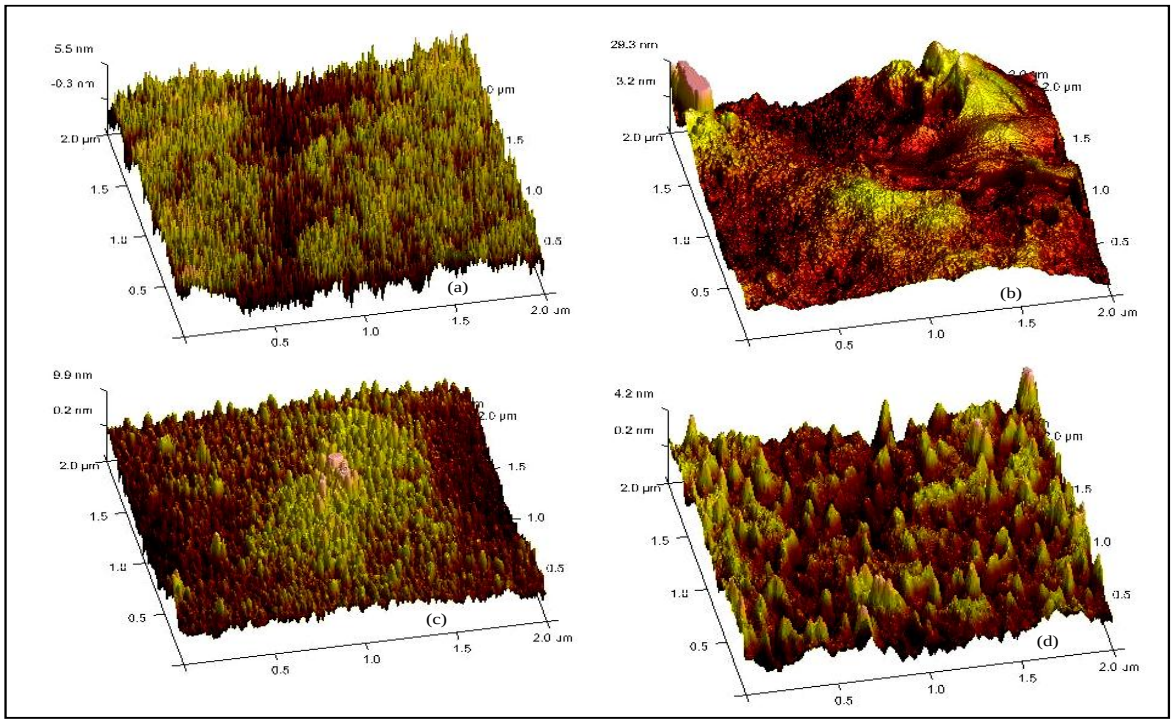

Figure 4: The AFM topography for (a) pristine glassy carbon and irradiated samples (b) fluence: 5.0E+11 ions/cm^2; E_k 460 keV (c) fluence: 6.2E+11 ions/cm^2; E_k 60 keV and (d) fluence: 1.0E+12 ions/cm^2; E_k 60 keV.

Table 2: Quantitative information extracted from the AFM analysis showing variation of surface of surface roughness, hillock size with varying irradiation parameters.

Sample ID	Fluence (Xe^{40+}/cm^2)	Potential energy (keV)	Kinetic energy (keV)	Surface roughness Rq (nm)	Max hillock height (nm)	Maximum hillock width (nm)
VGC	0	0	0	1.67		
GC2.3	5.0E+11	39	460	7.44	50.0	0.19
GC2.1	6.2E+11	39	060	2.60	09.9	0.20
GC1	1.0E+12	39	060	1.10	04.3	0.28

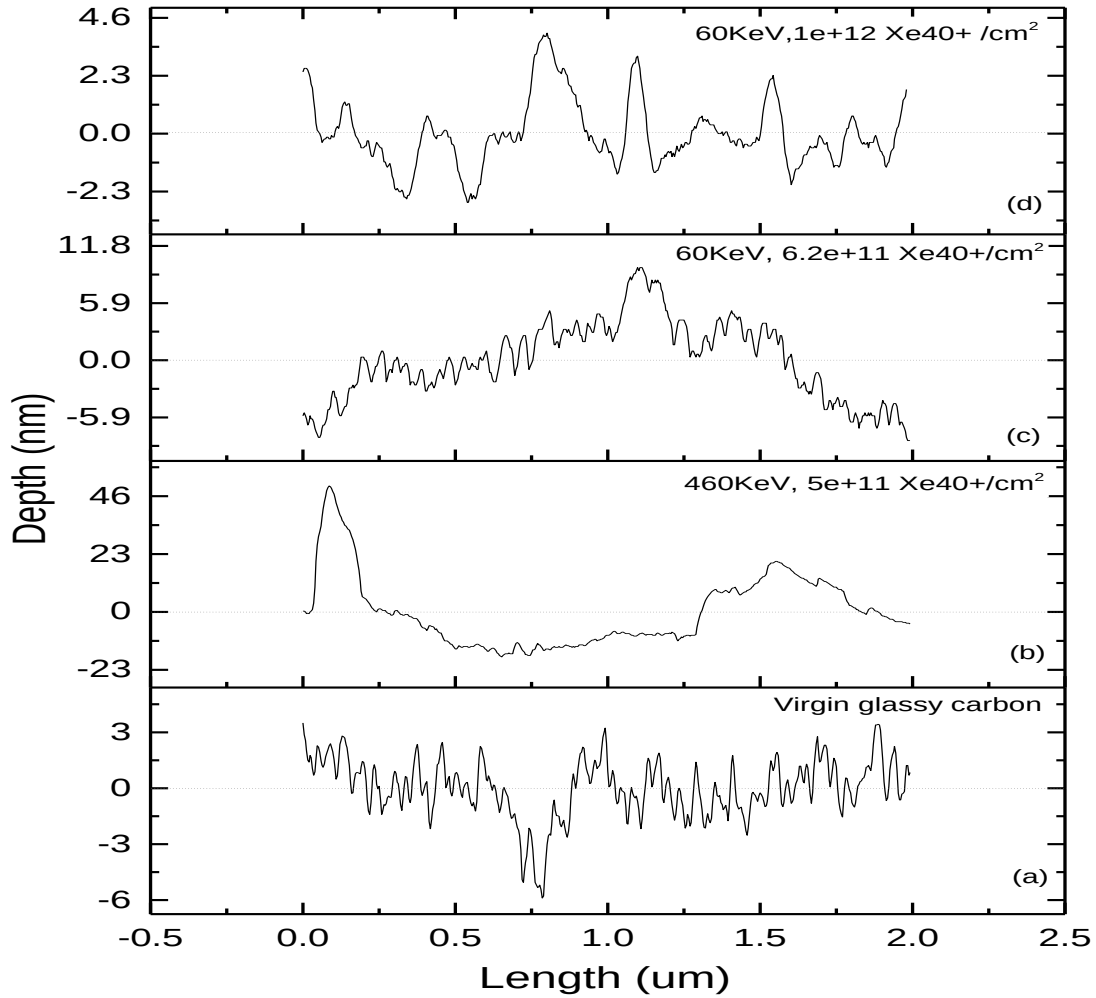

Figure 5: Cross-sectional view of the hillocks and surface roughness developed with fluence and kinetic energy of HCI.

CONCLUSION

The analysis of the behaviour of glassy carbon structure under Xe^{40+} HCI irradiation has been carried out with Raman spectroscopy and AFM. Raman results show that the virgin glassy carbon has a crystalline size of 2.91 nm. This parameter was found to have reduced in size due to increase in disorder introduced by the HCI irradiation. Samples irradiated with high kinetic energy of 460 keV has the least crystalline size of 1.54 nm. This shows that the energy of HCI contributes substantially to damage level introduced in glassy carbon. The AFM results concur with results obtained from Raman analysis. The hillock size and surface roughness are most pronounced in irradiated sample with kinetic energy of 460 keV. The reduction of the peaks ratio in addition to slight downshift of the G peak compared to G peak position of pristine glassy carbon sample is a sign that the glassy carbon structure experience disorder and subsequent accumulation of sp^3 atoms. As observed, there is only a slight shift in the D and G peak positions, which shows that the damage is only at minima level. This is attributed to the shielding role of the W films against the bombarding HCI. This finding indicates that W films enhance the radiation shield ability of glassy carbon.

REFERENCES

Al-Jishi, R., & Dresselhaus, G. (1982). Lattice-dynamical model for graphite. Physical Review B, 26(9): 4514-4522.

Antunes, E. F., Lobo, A. O., Corat, E. J., Trava-Airoldi, V. J., Martin, A. A., & Verı´ssimo, C. (2006). Comparative study of first- and second-order Raman spectra of MWCNT at visible and infrared laser excitation. Carbon, 44(11): 2202–2211.

Arnau, A., Aumayr, F., Echenique, P. M., Grether, M., Heiland, W., Limburg, J., Winter, H. P. (1997). Interaction of slow multicharged ions with solid surfaces. Surface Science Reports, 27(2): 113-239.

Aumayr, F., Facsko, S., El-Said, A. S., Trautmann, C., & Schleberger, M. (2011). Single ion induced surface nanostructures: A comparison between slow highly charged and swift heavy ions. Journal of Physics of Condensed Matter, 23(10): 39-45.

Bukalov, S. S., Leites, L., Sorokin, I., & Kotosonov, S. (2014). Structural changes in industrial glassy carbon as a function of heat treatment temperature according to raman spectroscopy and X-ray. Nanosystem, Physics, Chemistry and Mathematics, 5(1): 186–191.

Craievich, A. F. (1976). On the structure of glassy carbon. Material Research Bulletin, 11.

Das, S., Ohashi, H., & Nakamura, N. (2015). Study of interactions of slow highly charged bismuth ions with ZnO nanorods. Transaction of Indian Instrument and Methods, 1(3): 1-10.

Elman, B. S., Dresselhaus, M. S., Dresselhaus, G., Maby, E. W., & Mazurek, H. (1981). Raman scattering from ion-implanted graphite. Physical Review B, 24(3), 1027–1034.

Ferrari , A. C., & Robertson, J. (2001). Resonant Raman spectroscopy of disordered, amorphous and diamondlike carbon. Physical Review B, 64(6), 1–13.

Ferrari, A. C., & Robertson, J. (2000). Interpretation of Raman spectra of disordered and amorphous carbon. Physical Review B, 61(4): 14095–14107.

Friedrich, A., & Hannspeter, W. (2004). Potential sputtering. Philosophical Transaction of Royal Society of London, 362(8): 77–102.

Hlatshwayo, T. T., Sebitla, L. D., Njoroge, E. G., Mlambo, M., & Malherbe, J. B. (2017). Annealing effects on the migration of ion-implanted cadmium in glassy carbon. Nuclear Instruments and Methods in Physics Research B, 395(5): 34–38.

Innocent, A. J., Hlatshwayo, T. T., Njoroge, E. G., & Malherbe, J. B. (2018). Interface interaction of tungsten film deposited on glassy carbon under vacuum annealing. Vacuum, 148(3): 113-116.

Innocent, A. J., Hlatshwayo, T. T., Njoroge, E. G., Ntsoane, T. P., Madhuku, M., Ejeh, E. O., Malherbe, J. B. (2020). Evaluation of diffusion parameters and phase formation between tungsten films and glassy carbon. Vacuum, 175(3): 1-8.
McCulloch, D. G., Prawer, S., & HofFman, A. (1994). Structural investigation of xenon-ion-beam-irradiated glassy carbon. Physical Review B, 50(4): 5905–5917.
Meng, H., Julong, H., Zhisheng, Z., Timothy, A. S., Wentao, H., Dongli, Y., . . . Yongjun, T. (2017). Compressed glassy carbon: An ultrastrong and elastic interpenetrating graphene network. Science Advances, 3(1): 1-7.
Mingjie, L., Vasilii , I. A., Hoonkyung, L., Fangbo, X., & Boris, I. Y. (2013). Carbyne from first principles: Chain of C atoms, a nanorod or a nanorope? ASME, 7(2): 10075–10082.
Nathan, M. I., Smith, J. E., & Tu, K. N. (1974). Raman spectra of glassy carbon. Journal of Applied Physics, 45(1): 2370.
Njoroge, E. G., Sebitla, L. D., Theron, C. C., Mlambo, M., Hlatshwayo, T. T., Odutemowoyo, O. S., . . . Malherbe, J. B. (2017). Structural modification of indium implanted glassy carbon by thermal annealing and SHI irradiation. Vacuum, 144(2): 63–71.
Philipps, V. (2011). Tungsten as material for plasma-facing components in fusion devices. Journal of Nuclear Material, 415(4): S2–S9.
Raman, C. V., & Krishnan, K. S. (1928). A new class of spectra due to secondary radiation Part I. Indian Journal of Physics, 2(3): 399-419.
Schneider, D. H., & Briere, M. A. (1996). Investigations of the interactions of highest charge state ions with surfaces. Physica Scripta, 53(2): 228-242.
Sobota, D., Pajek, M., Skrzypiec, K., Mendyk, E., & Teodorczyk, M. (2017). Modification of gold and titanium nanolayers using slow highly charged Xe q+ ions. Nuclear Instruments & Methods in Physics Research B, 408(3): 235–240.
Tuinstra, F., & Koenig, J. L. (1970). Raman Spectrum of Graphite. Journal of Chemistry and Physics, 53(7): 1126-1130.